EDGE ARTICLE

Check for updates

Synthesis and characterisation of four bimetallic gold–gallium clusters with Au–Ga rings as a new structural motif in gold cluster chemistry†

Markus Strienz, Florian Fetzer and Andreas Schnepf ![ID] *

Using the newly introduced reducing agent in gold cluster chemistry GaCp, four new bimetallic gold–gallium cluster compounds were synthesised, stabilised by alkylphosphine ligands. The gold core of $Au_6(GaCl_2)_4(PEt_3)_6$, $Au_7(GaCl_2)_3(P^nPr_3)_6$ and $Au_{13}(GaCl_2)_5(GaCl)(P^nPr_2{}^nBu)_9$ is composed of two, three and four Au_4 tetrahedra, linked in different ways. This arrangement gives the last-mentioned cluster the shape of a five-pointed star. A fourth synthesised metalloid gold cluster $Au_{13}(GaCl_2)_5(P^nPr_3)_9$ consists of a voluminous gold core encircled by a gold–gallium chain. These gold–gallium chains are present in all four cluster compounds and are similar to the well-known gold–sulphur staple motifs in thiol-stabilised gold cluster compounds.

Introduction

While the famous polymath Michael Faraday already synthesized colloidal gold and investigated its properties hundreds of years ago, the precise structure and composition of gold colloids remained elusive for a long time.[1] This changed with progress in X-ray structure analysis and the synthesis and characterization of the first atomically precise gold cluster compound was realized by Malatesta in 1969.[2] Gold cluster compounds form a subgroup of nanoparticles, standing out by the knowledge of their atomically precise structure, which is enabled by crystallographic structure determination on single crystals. The first atomically precise gold cluster compound $Au_{11}(PPh_3)_7(SCN)_3$ can be described as a centered Au_{10}-centaur polyhedron. In the following years, a large number of further synthesized clusters revealed the immense diversity of structures in such compounds.[3,4] The platonic bodies of the tetrahedron within $Au_4(\mu\text{-I})_2(PPh_3)_4$,[5] the octahedron within $[Au_9\{P(p\text{-}C_6H_4Me)_3\}_8]^{3+}$[3] and the icosahedron within $[Au_{13}Cl_2(PMe_2Ph)_{10}]^{3+}$[6] should be highlighted. These basic motifs can be combined to create larger and more complex structures. An example is the $[Au_6(PPh_3)_6]^{2+}$ cluster, whose structure can be described by two tetrahedra connected by an edge.[7] Even larger cluster compounds can be described as agglomeration of smaller platonic bodies extending the widely used core–shell description.[8] Exemplarily, the structure of the $Au_{32}(R_3P)_{12}Cl_8$-cluster (R = Et, ^nPr, ^nBu) can be either described as Au_{12}-core in

the form of a distorted icosahedron enclosed by a shell of 20 gold atoms forming a pentagon dodecahedron.[9] Otherwise the structure can be seen as built by 20 Au_4-tetrahedra, each connected by three edges.[10]

By using thiol ligands, a new class of multi-shell gold cluster compounds with a wide variety of shapes and structural motifs is realized.[11] Most of these clusters are metalloid clusters as within these clusters more metal–metal than metal–ligand bonds are present and at least one metal atoms exist that is only bound to other metal atoms, leading to the general formulae (M_nL_m; $n > m$). The shell of thiol substituted metalloid gold clusters shows a new structural motif, the so called staple motif of the form $-SL-(Au-SL-)_n$ ($n = 1-4$). Dependent on the size of the cluster, larger and smaller staple motifs are realized.[12-15] Larger clusters like $Au_{279}(SR)_{84}$ or $Au_{144}(SR)_{60}$, which is protected by 30 equivalent RS–Au–SR units, tend to have shorter motifs.[14,15] In contrast, smaller clusters like $Au_{30}(SR)_{18}$ or $Au_{18}(SR)_{14}$, which is protected by an $Au_4(SR)_5$ chain, tend to have longer motifs.[12,13] In addition to the chains, gold clusters stabilized by rings of composition $(AuS)_4$ are also known.[16] The synthesis of all gold cluster compounds discussed so far is based on the reduction of a gold precursor with $NaBH_4$ or a similar reducing agent like $LiHB^sBu_3$. However, to further enhance the range of the synthesis it has been shown that other reducing agents can lead to gold cluster compounds with different structures and heteroatoms incorporated into the cores. For example, $[(PPh_3)_8Au_9GaCl_2]^{2+}$ is synthesized using the subvalent main group compound GaCp.[17] $[(PPh_3)_8Au_9GaCl_2]^{2+}$ consists of a gold core in form of a centaur polyhedron with a single $GaCl_2$ unit. Since it could be shown for systems with $NaBH_4$ as reducing agent that gold chlorides with aryl- or alkylphosphines as donors behave differently during the reduction, we wondered if this is also valid using GaCp as

Chemistry Department, Universität Tübingen, Auf der Morgenstelle 18, D-72076, Germany. E-mail: andreas.schnepf@uni-tuebingen.de

reducing agent.[2,9] In the following the results of the reduction of different alkyl–phosphine stabilized Au(I) precursors with GaCp are presented.

Results and discussion

Starting from (THT)AuCl (THT = tetrahydrothiophene), the weakly bound THT ligand can be replaced by a stronger binding phosphine ligand. In the presented work, the phosphines Et_3P, $^nPr_3P$ and $^nPr_2{}^nBuP$ were used, leading to the gold precursors $(Et_3P)AuCl$, $(^nPr_3P)AuCl$ and $(^nPr_2{}^nBuP)AuCl$. The reducing agent GaCp is prepared *in situ* from the metathesis reaction of "GaI" and NaCp about one hour before the reaction. During this time, the metathesis salt NaI can settle so that the GaCp solution can be filtered off and is used for the subsequent reduction without further purification.

$Au_6(GaCl_2)_4(PEt_3)_6$ 1

The reduction of $(Et_3P)AuCl$ with GaCp in toluene yields a dark red reaction solution. After removal of all volatiles, washing with pentane and extraction with toluene the smallest of the here presented cluster compounds $Au_6(GaCl_2)_4(PEt_3)_6$ **1** (see Fig. 1a) is obtained (1.3% yield). **1** crystallizes in the monoclinic crystal system in space group $C2/m$. The asymmetric unit of **1** consists of three gold atoms Au1, Au2 and Au3. The remaining gold atoms Au1′, Au1″ and Au1‴ are the result of symmetry

Fig. 1 (a) Molecular structure of **1** in the solid state. All atoms except for carbon are displayed as thermal ellipsoids with 50% probability. Hydrogen atoms are omitted for clarity. Au: gold, Ga: blue, P: violet, Cl: green. (b) Metallic core of **1** with the central edge connected tetrahedra highlighted by a polyhedral presentation.

operations. Within **1**, the six gold atoms are arranged as two Au_4-tetrahedra sharing one edge, resulting in D_{2h} symmetry (see Fig. 1b).

The motif of the edge sharing tetrahedra is well known for Au_6 cluster compounds. One example, $[Au_6(PPh_3)_6](SCN)_2$ has been published by Mingos in 1986.[7] Interestingly another Au_6-cluster compound, $[Au_6\{P(C_6H_4Me$-$o)Ph_2\}_6][BF_4]_2$, was synthesized using the also very uncommon reducing agent $Ti(\eta$-toluene$)_2$.[7] In addition to phosphines, thiolates were also used as ligands within $Au_6(STsi)_2(PPh_3)_4$ (Tsi $= C(SiMe_3)_3$).[18] The gold–gold bonds in **1** can be grouped into three categories based on their length (see Table 1). The shared bond of the two tetrahedra (Au2–Au3) is with 257.4 pm the shortest one. The length of the two terminal gold–gold bonds (Au1–Au1′ and Au1″–Au1‴) amounts to 274.6 pm. The other eight bond lengths are the longest ones with 301.9 ± 14.8 pm, exceeding the gold–gold distances in the bulk phase of gold (288 pm). The bond lengths vary thus by more than 50 pm between the shortest and the longest one. This difference is significantly smaller in the comparable gold clusters $[Au_6(PPh_3)_6](SCN)_2$ and $Au_6(STsi)_2(PPh_3)_4$, at about 20 pm.[7,18] Compared to these two structures, the length of the shared tetrahedral edge is slightly shorter, while the distance between the terminal gold atoms is higher, giving **1** a flatter shape (see Table 1). The gold core in **1** is surrounded by four $GaCl_2$ units. Two of these $GaCl_2$ units, Ga2 and Ga2′, are located in the cavity spanned by the two tetrahedra. As a result, each of the gallium atoms is bound to four gold atoms. To simplify the comparison of the different structural gold–gallium motifs presented in this publication, this Au_4GaCl_2 unit will be abbreviated as **d** (see Fig. 2 bottom right). The four horizontal Ga–Au bonds (*e.g.* Au1–Ga2) have a length of 260.4 pm, which corresponds to the length known in gallium–gold alloys.[19] The vertical Au–Ga bonds are significantly longer at 280.2 ± 16.4 pm. Two further $GaCl_2$ units bind to the outer edges of the tetrahedra with an Au–Ga-bond length of 251.5 pm each, forming a Au_2GaCl_2 unit a (see Fig. 2 top left). A similar bonding situation is known from **a** $[(dppe)_2Au_3In_3Cl_6(THF)_3]$ cluster in which an indium atom bridges a gold–gold bond to form an Au_2InCl_2THF unit and from a $[Au_3(\mu$-$GaI_2)_3(Cp*Ga)_5]$ cluster with three GaI_2 units, bridging a Au_3 triangle.[20,21] The gold–gallium distances in this cluster published by Sharp are 253.5 pm, almost the same length as in **1**. A gallium atom bridging a silver–silver bond is known from a $[Ga(C_6H_5Me)_2]_2$-$[Ag_4\{Ga(OTf)_3\}_4(\mu$-$Ga)_6(OTf)_4]$ cluster in which six $GaOTf_{2/3}$ units bridge the edges of an Ag_4 tetrahedron.[22] The average distances between the silver and the bridging gallium atoms are with 263 pm similar to the distances in **a**. To get a better understanding of the bonding situation, in special of the gold–gallium bonds, we calculated localized molecular orbitals (LMOs). Thereby, we found five 3c2e bonds, consisting of two gold atoms bridged by a gallium atom, similar to **a**. Two of the five 3c2e bonds are formed by the four terminal gold atoms (Au1–Au1′–Ga1 and Au1″–Au1‴–Ga1′). The other three 3c2e bonds are formed by Ga2 and Ga2′ with the six gold atoms (see Fig. 3 bottom). From a symmetrical reason an even number of orbitals would be expected, so the three orbitals result from the distortion of the cluster. The structural distortion is obvious from the different
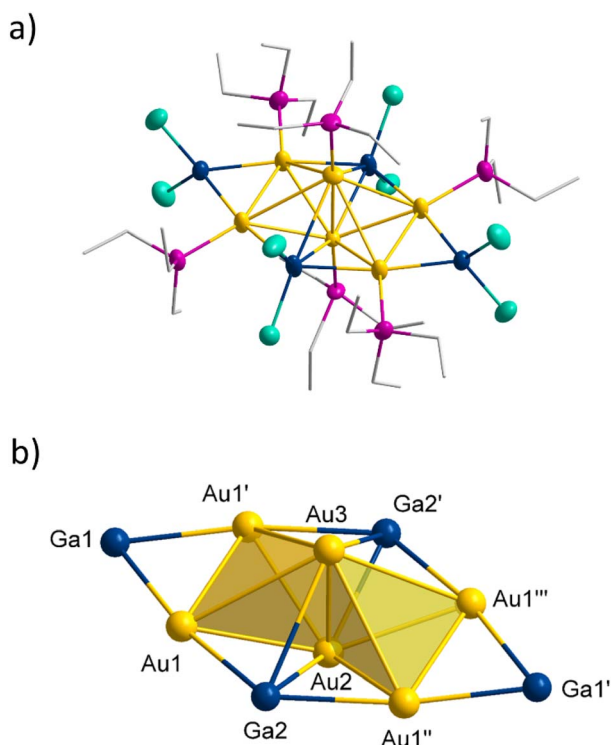
Table 1 Gold–gold binding lengths of 1, [Au$_6$(PPh$_3$)$_6$]$^{2+}$ and Au$_6$(STsi)$_2$(PPh$_3$)$_4$

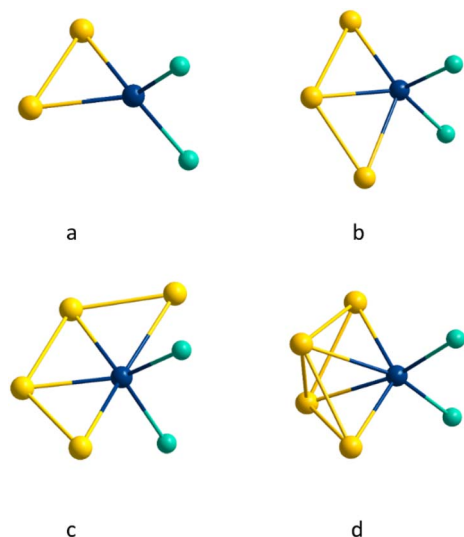| Bond length of	**1**	[Au$_6$(PPh$_3$)$_6$]$^{2+7}$	Au$_6$(STsi)$_2$(PPh$_3$)$_4$ (ref. 18)
Shared tetrahedral edge [pm]	257.4	265.1	263.8
Terminal gold bonds [pm]	274.6	266.6 ± 0.3	263.7
Bridging gold bonds [pm]	301.9 ± 14.8	279.1 ± 2.9	280 ± 2.7

Fig. 2 Images of the four different structural binding situations of the GaCl$_2$ units in **1–4**. Top left: Au$_2$GaCl$_2$ building motif **a**, subunit of **1**. Top right: Au$_3$GaCl$_2$ building motif **b**, subunit of **2**, **3** and **4**. Bottom left: Au$_3$GaCl$_2$ building motif **c**, subunit of **4**. Bottom right: Au$_4$GaCl$_2$ building motif **d**, subunit of **1**, **2** and **3**. Au: yellow, Ga: blue, Cl: green.
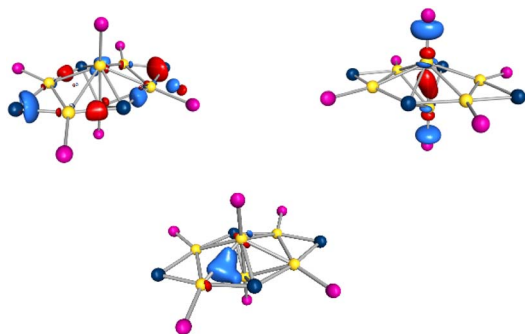

Fig. 3 Top: Calculated HOMO (left) and HOMO−4 (right) of **1**, based on the X-ray structure. Bottom: calculated LMO385 of **1**, based on the X-ray structure.

bond lengths to the bridging gold atoms (compare Au1″–Au3 with 326.9 pm and Au1′–Au3 with 299.1 pm). Thus, the reason for the large differences in terms of bond lengths of **1** compared to other Au$_6$ clusters is the presence of the gallium subunits.

1 is coordinated by a total of six PEt$_3$ ligands, so that every gold atom bears a ligand. Due to the high symmetry of **1** only two signals are observed within the ^{31}P-NMR spectrum (see SI†).

In order to further investigate the bonding situation, as well as to reveal a possible superatomic character, DFT calculations

were performed based on the crystal structure. We predict the electronic configuration of the cluster by assuming +1 electron for each gold atom, +1 electron for each GaCl$_2$ unit based on the assumption that gallium is gallium(III), and zero for the neutral phosphine ligands. Under these assumptions, the number of cluster electrons in **1** is 10, resulting from 6 electrons from the gold atoms and 4 additional electrons from the four GaCl$_2$ units. 10 is not an usual magic number, but it can be explained by an 1s^2, 1p^6, 2s^2 molecular orbital configuration. The HOMO–HOMO−4 show contributions of the gold and gallium atoms. Thereby, HOMO and HOMO−1 are mainly build by the GaCl$_2$ units and their neighbouring gold atoms (see Fig. 3 top left). The six electrons in the HOMO−2, HOMO−3 and HOMO−4 explain the already mentioned very short bond distances between the respective gold atoms. The Au2–Au3 bond in the HOMO−4 is visualized in Fig. 3 top right. The orbitals described can be separated in orbitals of a central Au$_2$ unit (HOMO−4) enclosed by an [AuGa]$_4$ chain (HOMO to HOMO−3). In the calculated orbitals there is thus no evidence of any delocalized orbitals, indicating that the bonding might be better described by localized bonds.

Au$_7$(GaCl$_2$)$_3$(P^{n}Pr$_3$)$_6$ 2

Using P^{n}Pr$_3$ instead of PEt$_3$ as stabilizing ligand for the Au(I)-precursor, the reduction of (^{n}Pr$_3$P)AuCl with GaCp in toluene yields a dark red solution. After workup and extraction of the dark red solid with pentane a second cluster species with the composition Au$_7$(GaCl$_2$)$_3$(P^{n}Pr$_3$)$_6$ **2** (see Fig. 4a) is obtained (yield 13.9%). **2** can be isolated as black crystals and crystallizes within the triclinic crystal system in space group $\bar{P}1$. The core structure of **2** is structurally related to the structure of **1** on tilting one tetrahedron around the central shared edge (Au1–Au6). The convergence of the two tetrahedral structures thereby leads to the formation of a new bond (Au3–Au4). This additional bond leads to the formation of another Au$_4$-tetrahedron and thus the core structure can be described as three face shared tetrahedra (see Fig. 4b). The bond shared by the three tetrahedra (Au1–Au6) is with 261.1 pm similar to the shared tetrahedral edge in **1** with 257.4 pm. The terminal gold bonds in **2** (Au2–Au3, Au3–Au4, Au4–Au5) are with 285.3 ± 5.5 pm slightly longer compared to **1**. The additional seventh gold atom (Au7) in **2** shows only one Au–Au bond (Au4–Au7), which is with 265.3 pm comparably short to the central Au–Au bond. The here realized arrangement of a Au$_6$-cluster, built from three shared tetrahedra is new for small gold cluster compounds. To the Au$_7$ core in **2** three GaCl$_2$ units are bound. These differ in the type of gold–gallium connection. Ga1 is bound in a similar way like **d** in **1**, forming a tetrahedra with Au1, Au5 and Au6. Comparable to
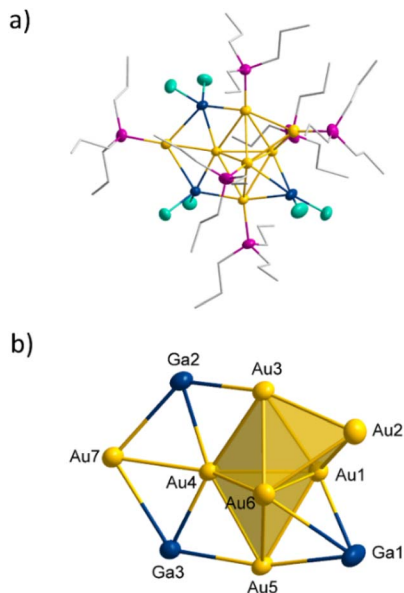
Fig. 4 (a) Molecular structure of **2** in the solid state. All atoms except for carbon are displayed as thermal ellipsoids with 50% probability. Hydrogen atoms are omitted for clarity. Au: yellow, Ga: blue, P: violet, Cl: green. (b) Metallic core of **2** with the three edge connected tetrahedra highlighted by a polyhedral presentation.

1, there are two short horizontal gold–gallium bonds (Au1–Ga1 and Au5–Ga1) with 250.1 pm and 264.6 pm, as well as a significantly longer vertical bond (Au6–Ga1) with 304.5 pm.

In contrast to **1**, there is no fourth bond between Au2 and Ga1 due to the large distance of 351.2 pm. A similar bonding situation is known from the earlier mentioned [(dppe)$_2$Au$_3$In$_3$-Cl$_6$(THF)$_3$] cluster, in which one indium atom is bonded to three gold atoms to form a Au$_3$In tetrahedron.[20] LMO calculations show, that this gold–gallium motif can be explained by a 3c2e bond and is more likely to the structural motif **a**. The other two gallium atoms Ga2 and Ga3 also bind to three gold atoms each. In this case, however, all three bonds are in one plane, leading to the formation of two edge shared Au$_3$GaCl$_2$ triangles **b** (see Fig. 2 top right). The middle of the three bonds is with 242.7 pm strikingly short (Ga2–Au4, Ga3–Au4). The two outer bonds are with 256.4 pm (Au3–Ga2) and 279.4 pm (Ga3–Au5) slightly longer than the ones in **a** and **d**. This structural motif is also found within the [(PPh$_3$)$_8$Au$_9$GaCl$_2$]$^{2+}$ cluster.[17] Again 3c2e bonds are found, resulting in a short central and longer outer gold–gallium interactions. **2** is coordinated by six P^{n}Pr$_3$ ligands, so that each gold atom binds a ligand, except Au4, to which the additional seventh gold atom is bound. Due to this gold atom being solely bound to metal atoms, **2** fulfils the definition of a metalloid cluster,[23] other than compound 1 in which every gold atom is bound to one ligand.

In **2**, only two of the phosphorus atoms in the cluster are identical due to the strong distortion. As a result, five different signals are found in the ^{31}P-NMR spectrum (see SI†). The intensities of the signals are 1 : 1 : 1 : 1 : 2, which is consistent with the molecular structure in the solid state, showing that the structure in solution is similar.
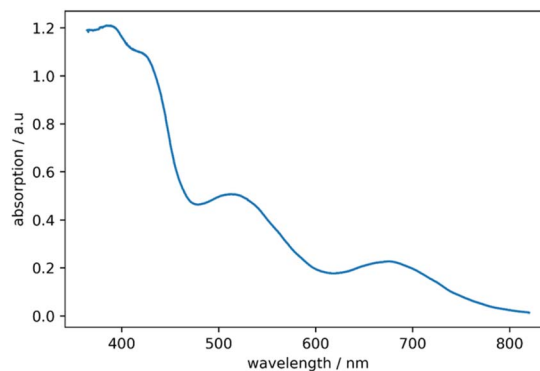

Fig. 5 UV/Vis spectrum of **2** in toluene. The spectrum shows three peaks at 384, 512 and 675 nm.

The number of cluster electrons in **2** is 10, resulting from 7 electrons from gold atoms and 3 electrons of GaCl$_2$ units. These ten electrons are located in the HOMO to HOMO−3 and HOMO−5. As in **1**, there are orbitals between the gold atoms themselves and orbitals emanating from the gold and gallium atoms, but no delocalized orbitals extending over a larger part of the cluster, so that one cannot speak of a superatom in **2** either. As in **1**, the highest-energy orbitals HOMO and HOMO−1 have portions of GaCl$_2$ units and their neighbouring gold atoms (see Fig. 6 top left). In addition, parts of the gold core are located in these two orbitals. The HOMO−3 of **2** is comparable to the HOMO−4 of **1** and shows a bond between the gold atoms spanning the common edge of the fused tetrahedra (see Fig. 6 top right).

The optical properties of **2** are investigated by UV-vis spectroscopy (see Fig. 5). A small peak is observed at 384 nm and a shoulder around 419 nm. The spectrum is similar to the UV/Vis spectrum of the comparable cluster compound [(PPh$_3$)$_8$-Au$_9$GaCl$_2$]$^{2+}$ in the near UV range, where absorption at 385 nm is also observed.[17] However, the UV/Vis spectrum of [(PPh$_3$)$_8$-Au$_9$GaCl$_2$]$^{2+}$ shows no signals with a wavelength higher than 405 nm. The spectrum of **2** shows two broad peaks, observed at wavelengths of 512 nm and 675 nm.
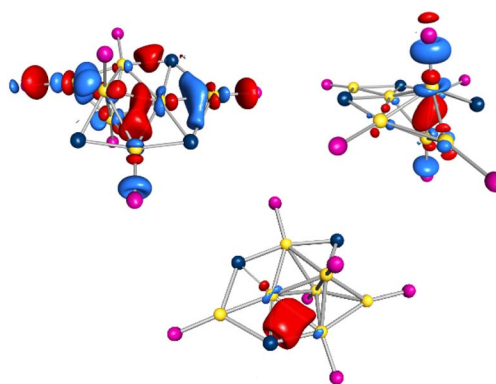

Fig. 6 Top: Calculated HOMO (left) and HOMO−3 (right) of **2**, based on the X-ray structure. Bottom: calculated LMO432 of **2**, based on the X-ray structure.

Since the yield of **2** is quite good and we know from the comparable Au_9GaCl_2 cluster, that the $GaCl_2$ unit can be easily abstracted, we attempted to modify the cluster so that it can be used as a molecular platform. Substitution of the chlorides by various lithium salts ($LiN(SiMe_3)_2$ and $LiSSi(SiMe_3)_3$) was unsuccessful and led to the decomposition of the cluster. The substitution of the $GaCl_2$ unit with an additional gold atom (Ph_3PAuCl) and the exchange with the heavier group 13 element indium ($InCl_3$) resulted in a colour change. Here is to mention, that calculations showed only small differences between $GaCl_2$ and $InCl_2$ as a building motif in a gold cluster.[24] Unfortunately, no product could be identified by NMR spectroscopy or single crystal X-ray diffraction.

$Au_{13}(GaCl_2)_5(GaCl)(P^nPr_2{}^nBu)_9$ **3**

In addition to **2**, another gold cluster of the composition $Au_{13}(GaCl_2)_5(GaCl)(P^nPr_3)_9$ can be crystallized from the pentane extract of the reaction of $(^nPr_3P)AuCl$ with GaCp. Due to very low quality of the crystals, the synthesis was repeated with the slightly modified $P^nPr_2{}^nBu$ ligand. The compound crystallizes in the monoclinic crystal system in space group $P2_1/n$ and could be

characterized as $Au_{13}(GaCl_2)_5(GaCl)(P^nPr_2{}^nBu)_9$ **3** (yield: 5.2%). The arrangement of the 13 gold atoms can be seen as a star whose five prongs are formed by a triangular and 4 tetrahedral subunits (see Fig. 7a). The gold atoms in **3** can be grouped in 4 smaller parts (see Fig. 7b). The biggest part is the two edge linked tetrahedra (yellow), already known from **1** and also in this case, the bonds can be grouped in three parts, according to their length. The Au–Au bond of the shared edge (Au1–Au2) is also here the shortest bond within **3** with 260.3 pm. The two terminal bonds (Au6–Au13 and Au7–Au12) are slightly longer with 269.2 ± 1.5 pm. The longest Au–Au bonds in this subunit are the bridging bonds with 300 ± 22.5 pm. The length of all these three bonds are nearly identical to the Au–Au lengths in **1** (see Table 2), resulting again in a flatter structure compared to other edge shared tetrahedral units. Two tetrahedral subunits (orange) are positioned diametrically opposed to the triangular face, connected *via* a shared gold atom (Au12, Au13). The Au–Au distances forming the edge lengths of the two Au_4 tetrahedra (Au3, Au5, Au10, Au13 and Au4, Au8, Au11, Au12) are nearly identical with average side lengths of 277.4 ± 2.3 and 277.3 ± 2.7 pm, respectively and are close to the Au–Au distances within $[(^tBu)_3PAu]_4{}^{2+}$ (271.4 ± 1.1 pm).[25] From each Au_4-tetrahedra one gold atom (Au10 and Au11) forms with an additional gold atom (Au9) a triangular face (violet). Like the neighbouring tetrahedra, the triangular face shows little distortion in the lengths of the sides with an average length of 271.4 ± 0.9 pm and bond angles of $60 \pm 0.3°$. There are five $GaCl_2$ units and one GaCl unit in **3**. Thereby, the five prongs of the gold core are all capped by one $GaCl_2$-unit. Four of these units are bound to three gold atoms, leading to the edge shared triangle motive **b**. Thereby, the central bond between the gold and the gallium atom is with 247 ± 0.9 pm (242.6 ± 0.2 pm in **2**) remarkably short. The two outer bonds are longer with 276.9 ± 5.2 pm (276.7 ± 9.8 pm in **2**). The fifth gallium atom capping the edge-linked tetrahedra binds to four gold atoms, forming motif **d** known from **1** with almost identical Au–Ga lengths. In the centre of the star formed by the gold atoms a single GaCl unit is found. This is bound to five gold atoms and forms the motif of a pentagonal pyramid with the gallium atom on the top with an average torsion angle of $29.4 \pm 2.3°$. The gold–gallium bonds are with an average bond length of 258.5 ± 0.8 pm very regular. A gallium atom, bound to five gold atoms is very unusual. A comparable arrangement of a $GaCl_2$ unit bound to 5 gold atoms is only known from $[Mo(AuPMe_3)_8(GaCl_2)_3(GaCl)][GaCl_4]$.[26] However, in this case the pentagonal pyramid is much more distorted, leading to average gold–gallium bonds of 286.7 ± 18.7 pm to the gold core within **3**.

The $GaCl_2$ and the GaCl unit differ also in their electronic situation. While the GaCl units in **3** tends to form three 3c2e
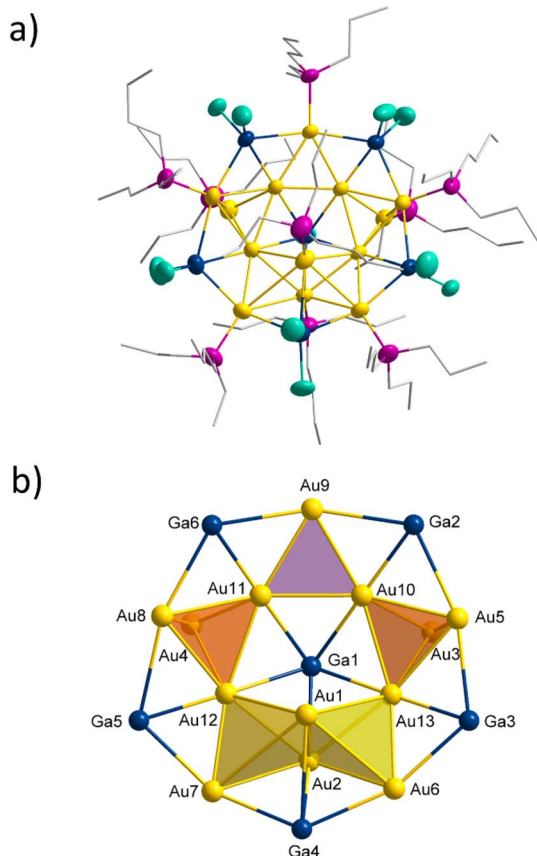

Fig. 7 (a) Molecular structure of **3** in the solid state. All atoms except for carbon are displayed as thermal ellipsoids with 50% probability. Hydrogen atoms are omitted for clarity. Au: yellow, Ga: blue, P: violet, Cl: green. (b) Core of **3** with the two edge connected tetrahedra (yellow), the two corner connected tetrahedra (orange) and the triangle face (violet) highlighted by a polyhedral presentation.

Table 2 Gold–gold binding lengths of 1 and 3

Bond length of	1	3
Shared tetrahedral edge [pm]	257.4	260.3
Terminal gold bonds [pm]	274.6	269.2 ± 1.5
Bridging gold bonds [pm]	301.9 ± 14.8	300 ± 22.5

bonds (Ga–Au1–Au12, Ga1–Au1–Au13, Ga1–Au10–Au11, figure top 9 left), similar to the 3c2e bonds in **1** and **2**, the $GaCl_2$ units form 2c2e bonds (*e.g.* Ga3–Au13, Fig. 9 top center). This is very interesting because despite the geometric similarity to **1**, the LMOs of **3** show a different electronic situation. The reason could be the electronic and sterical change due to the additional gold atoms, resulting in a more donor like behaviour of the $GaCl_2$ units, as seen in a gallium–uranium complex.[27]

Additionally 9 $P^nPr_2{}^nBu$ phosphines are coordinated, where each of the Au_4-subunits is coordinated by two phosphine ligands. A ninth phosphine is located at the terminal gold atom of the triangular face. Due to the low C_s symmetry of **3**, six chemically inequivalent phosphines are expected. The different signals can be identified in the ^{31}P-NMR spectra with an intensity ratio of 2 : 1 : 2 : 1 : 1 : 2 (see SI†) again showing that in solution the structure of the solid state is preserved.

If we keep the previous counting method, we get 18 electrons for **3**. In addition, the central GaCl unit should contribute 2 electrons, resulting in a total of 20 electrons for **3**. The five energetically highest orbitals have large proportions of the $GaCl_2$ units with their neighbouring gold atoms, as already seen in **1** and **2** (see Fig. 3 and 6). The combination of these orbitals gives the impression of two rings, where the outer one is equal to a $[AuGa]_5$ ring motif and the inner one is a five membered ring around the central gallium atom. The next, energetically lower orbitals, are dominated by the gold atoms. Despite the size of 13 gold atoms, there are no cluster orbitals in **3**. Instead the orbitals support the description of **3** as consisting of four smaller parts, namely the two edge shared tetrahedral, the two tetrahedral and the triangle. The formation of gold clusters composed of smaller units is well known in gold cluster chemistry. Tetrahedral Au_4 cluster can be connected *via* a vertex to form the bi-tetrahedral Au_7 kernel of a $Au_{20}(SPh^tBu)_{16}$ cluster or the tri-tetrahedral Au_{10} kernel of a $Au_{22}(SAdm)_{16}$ cluster.[28,29] An ensemble of Au_4 cluster have been assembled by Zn^{2+} ions forming a supercluster with interesting fluorescent properties.[30] This is also the explanation for the uncommon flat structure of **3**.

The optical properties of **3** have been investigated by UV-vis spectroscopy (see Fig. 8). Two broad peaks are observed at wavelengths of 406 nm and 493 nm and a smaller peak is at 638 nm. The optical spectrum is similar to the spectrum of **2**, which also shows three absorptions in the same region.
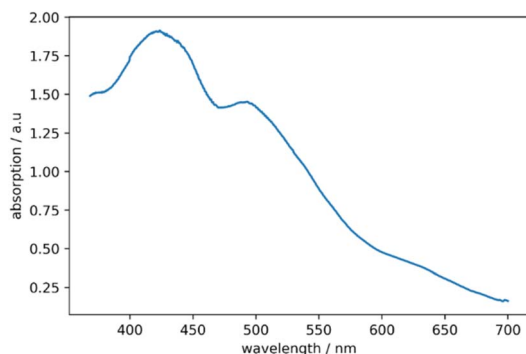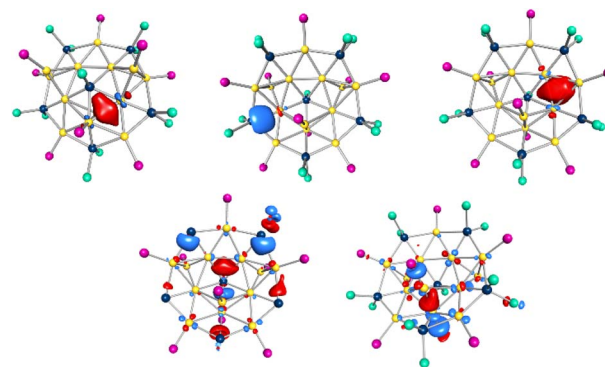

Fig. 9 Top: Calculated LMO751 (left), LMO747 (center) and LMO745 (right) of **3**, based on the X-ray structure. Bottom: calculated HOMO−1 (left) and HOMO−5 (right) of **3**, based on the X-ray structure.

$Au_{13}(GaCl_2)_5(P^nPr_3)_9$ 4

By repeating the reduction of $^nPr_3PAuCl$, it was possible to obtain another product of the reaction in crystalline form. However, this compound is not always isolable maybe due to the low yield of 0.55%. X-ray crystal structure analysis reveal that compound $Au_{13}(GaCl_2)_5(P^nPr_3)_9$ **4** has formed, crystallizing in the monoclinic crystal system in space group $P2_1/n$ (see Fig. 10a). The arrangement of the gold atoms in **4** can be divided
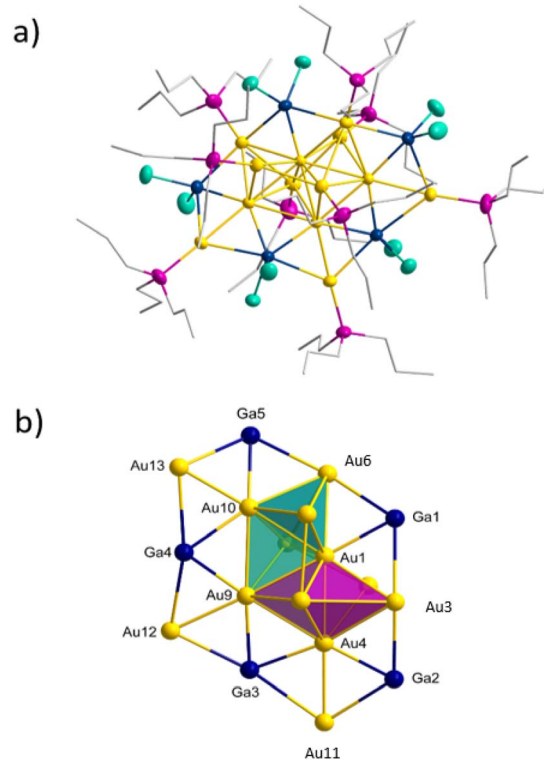

Fig. 10 (a) Molecular structure of **4** in the solid state. All atoms except for carbon are displayed as thermal ellipsoids with 50% probability. Hydrogen atoms are omitted for clarity. Au: yellow, Ga: blue, P: violet, Cl: green. (b) Gold and gallium atoms of **4**, both tetrahedral substructures are highlighted by a polyhedral representation (green and purple).

Fig. 8 UV/Vis spectrum of **3** in toluene. The spectrum shows three peaks at 406, 493 and 638 nm.

into two parts, a central core consisting of 10 gold atoms and three outer gold atoms surrounding this core. The ten central gold atoms form six tetrahedra, where three of the six tetrahedra are connected by a face and share two gold atoms (Au1–Au4 and Au1–Au10), thus forming two identical subunits (see Fig. 10b, green and violet). The three *via* face condensed tetrahedra is the structure of **2**. The two substructures are connected by the edge of two tetrahedra (Au1 and Au9). This gold core is reminiscent of a highly distorted icosahedron, which is missing 3 gold atoms. This is not surprising, since the icosahedron is a very common structural motif in gold cluster chemistry, either as a structure itself or as a core or shell in larger gold clusters.[31] Three gold atoms (Au11, Au12, Au13) bind to this central structure *via* the gold atoms Au4, Au9 and Au10. Here, the Au4–Au11 and Au10–Au13 bonds can be considered as an extension of the shared bond of the two subunits of the core, and Au9–Au12 as an extension of the bond between the two subunits.

The Au–Au distances to the outer gold atoms are with 262.3 ± 0.4 pm quite short and almost 20 pm less the Au–Au distance in elemental gold. The reason for this is in each case a 2c2e bond as visualized by LMO calculations (see Fig. 11 top right). There are 5 $GaCl_2$ units in **4**. Three of the gallium atoms (Ga1, Ga2, Ga5) bind to three gold atoms each forming the flat Au_3-$GaCl_2$ bonding motif **b**. Again, one bond is with 247.1 ± 0.9 pm clearly shorter than the other two with 271.2 ± 7.9 pm. Similar to **3**, these result from 2c2e bonds.

The gallium atoms Ga3 and Ga4 bind to four gold atoms each, forming a flat Au_4GaCl_2 unit **c** (see Fig. 2 bottom left). There are two short Au–Ga bonds at 251.3 ± 1.1 pm and two long Au–Ga bonds at 281.5 ± 5 pm in this building motif. Compared to the $GaCl_2$ units the cavity in **1** and **3**, all Au–Ga bonds in **4** are in one plane. Nevertheless, we see only strong interaction between a gold atom and a $GaCl_2$ subunit, the other short distances being enforced by the neighboring 2c2e gold bonds. It is possible that the additional gold and gallium atoms stabilize an Au_{10} intermediate, which is normally built up into an Au_{13} icosahedron. In **3** and **4**, the gold–gallium bonds appear to be more 2c2e bonds, while in the smaller cluster **1** and **2** the bonds are 3c2e bonds.
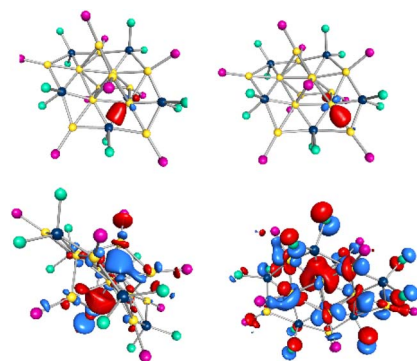

Fig. 11 Top: calculated LMO684 (left) and LMO680 (right) of **4**, based on the X-ray structure. Bottom: HOMO−1 (left) and HOMO−13 (right) of **4**, based on the X-ray structure.

The HOMO and the HOMO−4 in **4** are built by the outer gold atoms and the $GaCl_2$ units. HOMO−1 to HOMO−3 are delocalized over a large part of the cluster core and show a p type similar behaviour (see Fig. 11 bottom left). The remaining s type orbital is the HOMO−13 (see Fig. 11 bottom right). With an $1S^11P^6$ molecular orbital configuration and the 8 delocalized electrons, **4** can be described as a superatom-cluster. Still there is a separation needed, where only the core with 8 gold atoms shows this behaviour in opposite to more localized bonds within the Au_3Ga_5 chain. So **4** differs from **1–3**, as it shows delocalized cluster orbitals in the core, nevertheless it shows again a clear core-chain motive (*vide infra*). Within **4** nine P^nPr_3 ligands are coordinated to the cluster core. Therefore, the definition of a metalloid cluster is also fulfilled for this cluster.

Au–Ga chain motif

In the last few years, investigations on thiol-stabilized gold clusters have yielded a number of very different cluster species, varying both in the structure of their core and in their surrounding shell.[10] The shells of these compounds are usually composed of gold–sulfur chains, rings or both, whose stoichiometry and length can vary greatly. However, to our knowledge, such gold-main group element chain or rings are not known in gold cluster chemistry with any other element so far. All four gold–gallium clusters presented here are surrounded by a gold–gallium $[AuGa]_x$-chain, with the gold and gallium atoms alternating in order. There are four different structural building blocks of gallium atoms and their surroundings (**a**, **b**, **c**, **d**), which are already described above. The combination of these building blocks leads to an $[AuGa]_x$ chain (see Table 3). Consider that all $GaCl_2$ units in each of the clusters are part of the $[AuGa]_x$ chains, but not the GaCl unit in **3**. The length of the chains varies between the clusters. The shortest of the chain motifs is found in **2** with a six-member chain of composition $[AuGa]_3$ (see Fig. 12, top right). This chain is composed of two **b** units and one distorted **a**-motive. The average bond length between the gold and the gallium atoms in this chain is 267.8 ± 9.1 pm. Unlike the other three GaAu-chains, this chain is not closed and forms no ring. The chain in **1** has the shape of a nearly planar $[AuGa]_4$ ring (see Fig. 12, top left). It consists of two **d** and two **a** motifs in alternating order. The gold–gallium distances in this chain are with 255.9 ± 4.5 pm the shortest ones. The interior angles of the rings are 134.1 ± 42.7°. Of note are the widely varying bond angles in **1**, resulting from an alternation of fragments with small (97.7°) and large bond angles (170.2°). As a result, the ring of **1** has a rhombic shape with quasi-linear Ga–Au–Ga motifs. A 10-membered $[AuGa]_5$ chain is found in each of the Au_{13} clusters **3** and **4** (see Fig. 8, bottom). They are nearly identical with an average bond length of 276 ± 5.1 pm for **3** and 276.5 ± 7.4 pm for **4**. Thus, the distances are about 20 pm longer than for **1**. The internal angles of the rings are very similar: 141.7 ± 17° for **3** and 132.8 ± 21.3° for **4**. A similar alternation of short and wide bond angles as in **1** is also found in **3** and **4**, although here the differences are less pronounced. The properties of the $[AuGa]_x$-chains are directly related to the building blocks from which they are constructed,

Table 3 Number of links, average binding length, average angle and composition of the $[AuGa]_x$ chains in **1**, **2**, **3** and **4**

Cluster	1	2	3	4
Member amount of the chain	8	6	10	10
Average binding length [pm]	255.9 ± 4.5	267.8 ± 9.1	276 ± 5.1	276.5 ± 7.4
Average angle [°]	134.1 ± 42.7	131.7 ± 21.3	141.7 ± 17	132.8 ± 21.3
a Au_2GaCl_2	2	—	—	—
b Au_3GaCl_2	—	2	5	3
c Au_4GaCl_2 (flat)	—	—	—	2
d Au_4GaCl_2 (cavity)	2	1	1	—
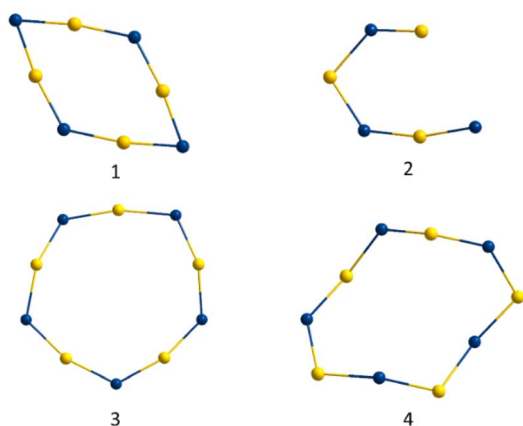
Fig. 12 $[AuGa]_x$ chains of **1**, **2**, **3** and **4**. The gold atoms are yellow and gallium atoms are blue.

which are determined by the electronic situation in the motifs themselves. The cavity building unit **d**, a composition of two 3c2e bonds, leads to large angles and short Au–Ga bond lengths. In contrast, within the smallest building block **a**, a single 3c2e bond leads to a small Au–Ga–Au angle and also short bond lengths. The combination of two building blocks **a** and **d** in alternating sequence in **1** results in a $[AuGa]_4$ chain with strongly alternating internal angles and short bond lengths. Within the building blocks **b** and **c**, as found in **3** and **4** the bond of the chain to the core is almost entirely correlated to 2c2e bonds with a sigma donor like behaviour and fewer interactions with the neighbouring gold atoms. This results in very long Au–Ga distances within the chain for **3** and **4**. In contrast to **1**, when two similar building blocks are used, the variation in length and angles for **3** and **4** is very small.

Comparison of different stabilized gold clusters shows that the $[AuGa]_x$ chain is very often present as a ring, whereas most of the known thiol-stabilized gold clusters are stabilized by a SR–[Au–SR]$_x$ chain. The length of the $[AuGa]_x$ chains is comparable to the chain length of the smaller thiol-stabilized gold clusters. Six $–Au_2(SR)_3–$ (R = SCH_2CH_2Ph) staples stabilize the Au_{13} core of a $[Au_{25}(SCH_2CH_2Ph)_{18}]^-$ cluster.[32] An $Au_{20}(SPh^tBu)_{16}$ cluster with an Au_7 core in the form of two vertex shared tetrahedra is even stabilized by a octametric gold–sulfur ring and additional trimeric and monomeric staples.[28] Whether the length of the $[GaAu]_x$ chain also decreases with increasing cluster size, similar to thiolate stabilized gold cluster, cannot be

assessed at present, since sufficiently large gold–gallium clusters are not yet synthesized.[10]

Conclusions

In this article, the synthesis of four intermetallic gold–gallium clusters has been reported. Crystals of all four cluster species can be obtained after work-up from the reduction reaction of a phosphine stabilized gold chloride with GaCp. The gold core of the smallest compound $Au_6(GaCl_2)_4(PEt_3)_6$ consists of two edge linked tetrahedra, a motif already known from other Au_6-clusters. The distorted edge linked tetrahedra is also part of the bigger $Au_7(GaCl_2)_3(P^nPr_3)_6$ cluster. The $Au_{13}(GaCl_2)_5$-$(GaCl)(P^nPr_2^nBu)_9$ cluster has a remarkable form of a star, where the 5 tips are formed by four Au_4-tetrahedra and an Au_3-triangular face, resulting in a very unusual flat shape. The fourth cluster $Au_{13}(GaCl_2)_5(P^nPr_3)_9$ consists of a gold core in form of two three edge shared tetrahedra and an enclosing AuGa-ring. These $[AuGa]_x$ ($x = 3–5$) chains are also found in all other cluster and allow a geometric separation of all cluster in a core and an enclosing ring, what is supported by DFT calculations. The $GaCl_2$ units are bound to the gold atoms via 3c2e or 2c2e bond. These rings are comparable to the Au–S ring and chain motifs in thiol-stabilised gold clusters, but have never been observed with other elements.

Data availability

The ESI† contains all detailed synthetic procedures, all spectroscopy, characterization data, and computational data. Structures are available on CCDC.

Author contributions

M. S.: cluster synthesis, quantum chemical calculations, writing. F. F.: cluster synthesis. A. S.: project administration, review & editing, supervision, funding acquisition.

Conflicts of interest

There are no conflicts to declare.

Acknowledgements

Notes and references

1 M. Faraday, *Phil. Trans.*, 1857, 145.

2 M. McPartlin, R. Maso and L. Malatesta, *J. Chem. Soc. D*, 1969, **7**, 334.

3 P. L. Bellon, F. Cariati, M. Manassero, L. Naldini and M. Sansoni, *J. Chem. Soc. D*, 1971, 1423.

4 J. W. A. Van der Velden, J. J. Bour, W. P. Bosman and J. H. Noordik, *Inorg. Chem.*, 1983, **22**, 1913.

5 F. Demartin, M. Manassero, L. Naldini, R. Ruggeri and M. Sansoni, *J. Chem. Soc., Chem. Commun.*, 1981, **5**, 222.

6 C. E. Briant, B. R. C. Theobald, J. W. White, L. K. Bell, D. M. P. Mingos and A. J. Welch, *J. Chem. Soc., Chem. Commun.*, 1981, **5**, 201.

7 C. E. Briant, K. P. Hall, D. M. P. Mingos and A. C. Wheeler, *J. Chem. Soc., Dalton Trans.*, 1986, **3**, 687.

8 N. Xia and Z. Wu, *Chem. Sci.*, 2020, **12**, 2368.

9 S. Kenzler, F. Fetzer, C. Schrenk, N. Pollard, A. R. Frojd, A. Z. Clayborne and A. Schnepf, *Angew. Chem., Int. Ed.*, 2019, **58**, 5902.

10 S. Kenzler and A. Schnepf, *Chem. Sci.*, 2021, **12**, 3116.

11 (*a*) P. D. Jadzinsky, G. Calero, C. J. Ackerson, D. A. Bushnell and R. D. Kornberg, *Science*, 2007, **318**, 430; (*b*) I. Chakraborty and T. Pradeep, *Chem. Rev.*, 2017, **117**, 8208; (*c*) R. Jin, C. Zeng, M. Zhou and Y. Chen, *Chem. Rev.*, 2016, **116**, 10346; (*d*) H. Qian, M. Zhu, Z. Wu and R. Jin, *Acc. Chem. Res.*, 2012, **45**, 1470.

12 A. Das, C. Liu, H. Y. Byun, K. Nobusada, S. Zhao, N. Rosi and R. Jin, *Angew. Chem., Int. Ed.*, 2015, **54**, 3140.

13 D. Crasto, S. Malola, G. Brosofsky, A. Dass and H. Häkkinen, *J. Am. Chem. Soc.*, 2014, **136**, 5000.

14 O. Lopez-Acevedo, J. Akola, R. L. Whetten, H. Grönbeck and H. Häkkinen, *J. Phys. Chem. C*, 2009, **113**, 5035.

15 N. A. Sakthivel, S. Theivendran, V. Ganeshraj, A. G. Oliver and A. Dass, *J. Am. Chem. Soc.*, 2017, **139**, 15450.

16 (*a*) S. Kenzler, C. Schrenk and A. Schnepf, *Angew. Chem., Int. Ed.*, 2017, **56**, 393; (*b*) S. Kenzler, C. Schrenk, A. R. Frojd, H. Häkkinen, A. Z. Clayborne and A. Schnepf, *Chem. Commun.*, 2018, **54**, 24.

17 F. Fetzer, C. Schrenk, N. Pollard, A. Adeagbo, A. Z. Clayborne and A. Schnepf, *Chem. Commun.*, 2021, **57**, 3551.

18 S. Kenzler, M. Kotsch and A. Schnepf, *Eur. J. Inorg. Chem.*, 2018, **2018**, 3840.

19 H. Pfisterer and K. Schubert, *Int. J. Mater. Res.*, 1950, **41**, 358.

20 F. P. Gabbai, A. Schier, J. Riede and H. Schmidbaur, *Inorg. Chem.*, 1995, **34**, 3855.

21 U. Anandhi and P. R. Sharp, *Angew. Chem., Int. Ed.*, 2004, **43**, 6128.

22 J. Boronski, M. Stevens, B. van IJzendoorn, A. Whitwood and J. Slattery, *Angew. Chem., Int. Ed.*, 2021, **60**, 1567.

23 A. Purath, R. Köppe and H. Schnöckel, *Angew. Chem., Int. Ed.*, 1999, **38**, 2926.

24 N. Pollard and A. Clayborne, *Understanding the Impact of Composition on the Geometry, Electronic Structure and Spectroscopic Profile of an Atomically Precise Gold-Phosphine Cluster*, DOI: **10.21203/rs.3.rs-2231969/v1**.

25 E. Zeller, H. Beruda and H. Schmidbaur, *Inorg. Chem.*, 1993, **32**, 3203.

26 A. Puls, P. Jerabek, W. Kurashige, M. Förster, M. Molon, T. Bollermann, M. Winter, C. Gemel, Y. Negishi, G. Frenking and R. A. Fischer, *Angew. Chem., Int. Ed.*, 2014, **53**, 4327.

27 S. Liddle, J. McMaster, D. Mills, A. Blake, C. Jones and W. Woodul, *Angew. Chem., Int. Ed.*, 2009, **48**, 1077.

28 C. Zeng, C. Liu, Y. Chen, N. L. Rosi and R. Jin, *J. Am. Chem. Soc.*, 2014, **136**, 11922.

29 Q. Li, S. Yang, T. Chen, S. Jin, J. Chai, H. Zhang and M. Zhu, *Nanoscale*, 2020, **12**, 23694.

30 H. Chang, N. Karan, K. Shin, M. Bootharaju, S. Nah, S. Chae, W. Baek, S. Lee, J. Kim, Y. Son, T. Kang, G. Ko, S. Kwon and T. Hyeon, *J. Am. Chem. Soc.*, 2021, **143**, 326.

31 (*a*) A. Dass, S. Theivendran, P. R. Nimmala, C. Kumara, V. R. Jupally, A. Fortunelli, L. Sementa, G. Barcaro, X. Zuo and B. C. Noll, *J. Am. Chem. Soc.*, 2015, **137**, 4610; (*b*) C. E. Briant, B. R. C. Theobald, J. W. White, L. K. Bell, D. M. P. Mingos and A. J. Welch, *J. Chem. Soc., Chem. Commun.*, 1981, 201.

32 M. W. Heaven, A. Dass, P. S. White, K. M. Holt and R. W. Murray, *J. Am. Chem. Soc.*, 2008, **130**, 3754.